ADVANCED FUNCTIONAL MATERIALS
www.afm-journal.de

Skyrmion Lattice Phases in Thin Film Multilayer

Jakub Zázvorka, Florian Dittrich, Yuqing Ge, Nico Kerber, Klaus Raab, Thomas Winkler, Kai Litzius, Martin Veis, Peter Virnau, and Mathias Kläui**

Phases of matter are ubiquitous with everyday examples including solids and liquids. In reduced dimensions, particular phases, such as the 2D hexatic phase and corresponding phase transitions occur. A particularly exciting example of 2D ordered systems are skyrmion lattices, where in contrast to previously studied 2D colloid systems, the skyrmion size and density can be tuned by temperature and magnetic fields. This allows for the system to be driven from a liquid phase to the onset of a hexatic phase as deduced from the analysis of the hexagonal order. Using coarse-grained molecular dynamics simulations of soft disks, the skyrmion interaction potentials are determined, and it is found that the simulations are able to reproduce the phase behavior. This shows that not only the static behavior of skyrmions is qualitatively well described in terms of a simple 2D model system but skyrmion lattices are versatile and tunable 2D model systems that allow for studying phases and phase transitions in reduced dimensions.

1. Introduction

Magnetic skyrmions, topologically stabilized whirls of magnetization, are in the focus of the scientific community due to their attractive properties for possible novel functional devices.[1–3] Using spin-transfer torque and spin–orbit torque,[4–7] skyrmions can be moved with high speeds at low current densities and can even be stabilized with no external magnetic field applied,[7–9] which makes them potentially useful for memory and computer logic devices.[3,10] In addition to such devices based on the controlled operation of single skyrmions, also thermally activated skyrmions and skyrmion ensembles have been suggested for functional devices for non-conventional computing approaches: recently it was shown, that skyrmions, including ensembles, can be relevant for stochastic computing where a functional skyrmion reshuffler device was implemented.[11] And in particular for reservoir computing, we have suggested to use ensembles of many skyrmions where the skyrmion interaction and collective behavior is of key importance.[12] Thus advanced functionality in nanoscale devices is enabled if the properties of ensembles of skyrmions can be understood and controlled. Periodic ensembles called skyrmion lattices have been found widely in bulk materials with B20 symmetry, where the topological structures are stabilized due to bulk Dzyaloshinskii–Moriya interaction (DMI).[4,5,13,14] However, in bulk systems the skyrmions are mostly not 2D like, as the "skyrmion tube" length can easily exceed the skyrmion diameter or even the skyrmion-skyrmion distance. In advanced thin film systems, skyrmions down to sub-nm thickness and diameters in the range of micrometers are stabilized, making them prime candidates for perfectly 2D systems. While skyrmion lattices have been studied theoretically in such systems, only recently first experimental reports of thin film lattices have been reported, albeit with systems where the relatively large (≈100 nm) film thickness is similar to the lateral skyrmion size making these systems not necessarily 2D.[13,15–17] Thus to experimentally probe the rich phase behavior of 2D systems[18–20] akin to colloids in the past,[21–23] 2D skyrmion lattices occurring in ultra-thin film stacks might be an ideal model system.[24] The nature of phase transitions in 2D systems of hard and soft disks has been a grand challenge in statistical physics, which has recently been numerically treated.[18] Apart from a liquid at low and a solid phase at high density, a third intermediate phase may emerge: The hexatic phase is characterized by short range translational and quasi-long range orientational order, and there is a clear need for experimental 2D systems to probe this unique phase behavior. This calls for studying 2D skyrmion lattices and analysis of their phase behavior with numerical simulations based on coarse-grained models from Statistical Mechanics to identify possibly unique 2D properties as well as gauge the suitability of these systems to study the exciting 2D phase behavior.

Dr. J. Zázvorka, F. Dittrich, Y. Ge, N. Kerber, K. Raab, T. Winkler, Dr. K. Litzius, Dr. P. Virnau, Prof. M. Kläui
Institute of Physics
Johannes Gutenberg-Universität Mainz
Staudingerweg 7, Mainz 55128, Germany
E-mail: virnau@uni-mainz.de; klaeui@uni-mainz.de

Dr. J. Zázvorka, Dr. M. Veis
Institute of Physics
Faculty of Mathematics and Physics
Charles University
Ke Karlovu 5, Prague 12116, Czech Republic

N. Kerber, Dr. K. Litzius, Dr. P. Virnau, Prof. M. Kläui
Graduate School of Excellence Materials Science in Mainz
Johannes Gutenberg-Universität Mainz
Staudingerweg 9, Mainz 55128, Germany

Dr. K. Litzius
Modern Magnetic Systems
Max Planck Institute for Intelligent Systems
Heisenbergstrasse 3, Stuttgart 70569, Germany

The ORCID identification number(s) for the author(s) of this article can be found under https://doi.org/10.1002/adfm.202004037.

DOI: 10.1002/adfm.202004037

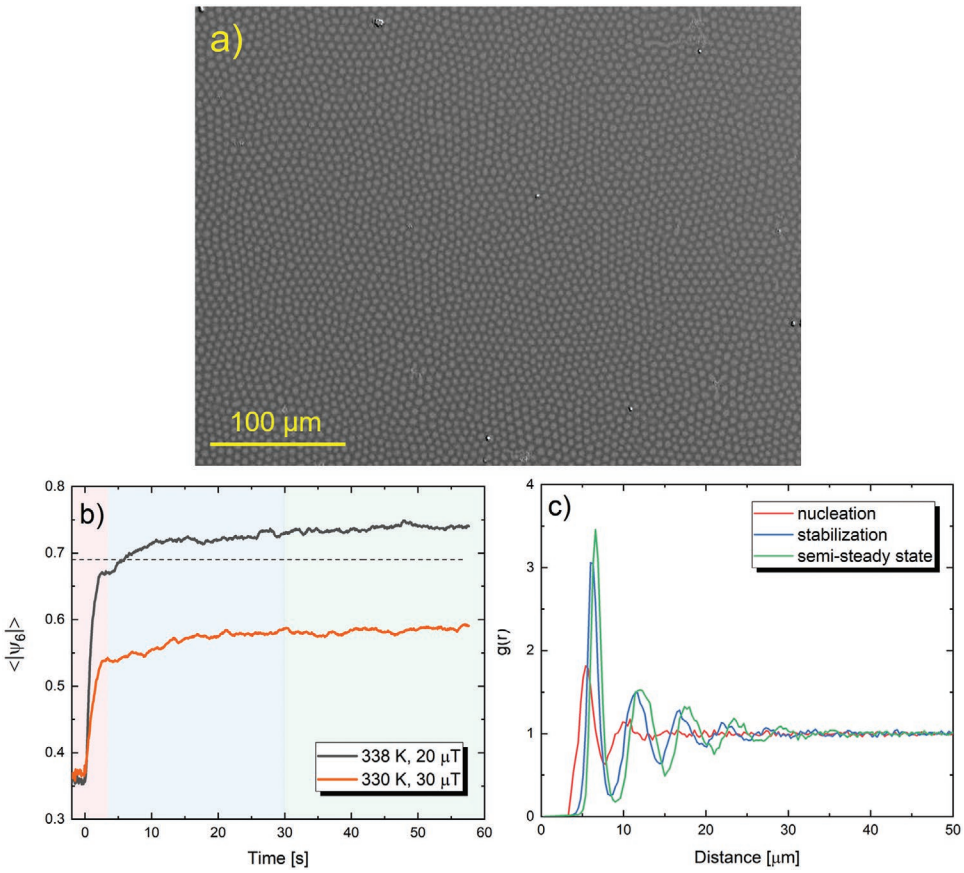

Figure 1. Picture of skyrmion lattice and evolution of phase quantifiers. a) Kerr image of a skyrmion lattice at 335 K with µm sized skyrmions. b) The evolution of $\langle|\psi_6|\rangle$ averaged over all skyrmions in one frame in dependence of time after nucleation. The red, blue, and green backgrounds depict the nucleation, stabilization, and a semi-steady skyrmion state, respectively. $\langle|\psi_6|\rangle$ is dependent on the temperature and the applied out-of-plane field. c) Pair correlation function $g(r)$ right after nucleation, in the stabilization phase and in the semi-steady state for temperature 338 K and 20 µT applied out-of-plane field. After switching off the in-plane field and the resulting skyrmion nucleation, the red pair correlation function (in (c)) emerges and indicates typical nearest and next-nearest neighbor distances. Blue and green curves show the pair correlation function $g(r)$ in the relaxation and semi-steady state of the lattice, respectively. In the stabilization process, the correlation function is noisier, whereas in the semi-steady state the function has a finer distribution.

Thus, in this work, we use a sub-nm thick CoFeB-based multilayer system to study the emergence of skyrmion lattices as well as their response to tuning external parameters such as temperature and field. Since the skyrmion diameter (**Figure 1**a) is three orders of magnitudes larger than its thickness (0.9 nm), and as the thickness of the magnetic layer is much smaller than the exchange length so that the magnetization texture is uniform along the z-direction, this system could be considered to be inherently 2D. This is distinctly different from previous reports on topologically trivial bubbles for instance in yttrium iron garnet (YIG) films that are >µm thick and where no sizeable DMI is found. By experimentally ascertaining the phase transitions, we demonstrate the 2D nature of the system as well as its suitability as a model system to probe 2D phase behavior.

2. Results and Discussion

Using Kerr microscopy imaging we investigated a low-pinning multilayer stack Ta(5)/$Co_{20}Fe_{60}B_{20}$(0.9)/Ta(0.08)/MgO(2)/Ta(5) similar to a material previously characterized in which the skyrmions show thermally activated diffusion at low skyrmion densities.[11] The studied material exhibits perpendicular magnetic anisotropy (PMA) and interfacial DMI.[11] Using out-of-plane magnetic field sweeps, stripe domains, and a low density of skyrmions are present in the sample. Upon fixing the out-of-plane field and a subsequent saturation of the sample using an in-plane field in any direction, a high density of skyrmions is nucleated in the sample when the in-plane field is reduced back to zero abruptly by switching off the power supply to the in-plane coil. Due to the interfacial DMI and concluded from current induced motion experiments, the observed skyrmions were topologically stabilized, with a fixed chirality, and rotational symmetry and a topological charge $Q = 1$. This is desired for our further investigation as there are no reports indicating phase transitions with spatially ordered $Q = 0$ magnetic bubbles that are not rotationally symmetric. The density and the mean radius of the skyrmions is controlled by the values of the out-of-plane magnetic field applied and the temperature. For details on the MOKE hysteresis loops and skyrmion lattice nucleation, see Supporting Information. By varying the out-of-plane field, the size and as a result also the skyrmion lattice density and

ordering is tuned, which is a unique handle compared to previously used systems, such as colloids with fixed sizes. Variations in temperatures are found to tune the amount of thermally activated motion but also the average skyrmion radius, as well as lattice density due to the changing magnetic properties.[11] To evaluate phases in 2D systems such as the skyrmion lattice phases (Figure 1a), we employ two quantifiers:

The local orientational order parameter[18,25] (Figure 1b)

$$\psi_6(k) = \frac{1}{n_k}\sum_{l=1}^{n_k} e^{i6\theta_{kl}} \tag{1}$$

and the pair correlation function (Figure 1c)

$$g(r) = \frac{1}{2\pi r}\frac{1}{N\rho}\sum_{k=1}^{N}\sum_{k\neq l}^{N}\langle\delta(r-|r_k - r_l|)\rangle \tag{2}$$

The local orientational order parameter is a standard measure to quantify the emergence of local hexagonal order.[18,25] θ_{kl} describes the angle of the connecting line between a (central) skyrmion k and the lth of its n_k nearest neighbors with respect to a fixed axis (here the x-axis).[18] The cut-off distance to find the nearest neighbors was selected to be the position of the first minimum in the corresponding pair correlation function $g(r)$. A strict cut is implemented, so the number of neighbors n_k will usually but not necessarily be 6. For a perfect (periodic) triangular lattice, the contribution of all six neighbors yields $|\psi_6| = 1$.

The 1D pair correlation function $g(r)$ (Equation (2)) contains basic information such as typical nearest and next-nearest neighbor distances and the general structure of a gas, liquid or crystal. Particularly, it allows us to quantify the local structure of a skyrmion lattice in area A by comparing it to a structureless, homogeneous fluid of area density $\rho = \frac{N}{A}$. Essentially, we count the number of particles located at a certain distance around each particle and divide this number by the expected number of particles in a fluid with no structure. In our modelling approach we use this quantifier to reproduce the basic structure of the system while keeping the fitting procedure manageable. Equation (2) is, however, not suited to visualize the emergence of hexagonal order like the 2D-pair correlation function, for example, used in ref. [18].

To study the evolution of the phases of the system, we take a video using the Kerr microscope after an in-plane magnetic field is switched off. The observed skyrmions are tracked, their positions are evaluated, and quantifiers are calculated for each frame in the video. Calculation of the correlation functions and individual skyrmion position evaluation is described in Section 4. The local orientational order parameter is calculated for every skyrmion in one frame except for those on the border of the frame. Note that in this context the expression "order parameter" refers to a parameter which quantifies the local orientational order of a system and is not to be understood in the classical sense as a parameter which characterizes second-order phase transitions. To obtain a quick indication of the state and the phase of the system, we introduce a heuristic parameter $\langle|\psi_6|\rangle$, which averages the absolute value of ψ_6 over all skyrmions for which ψ_6 was computed.[25] From simulations of a soft disc system we find that the liquid branch of the liquid to hexatic coexistence region is marked by $\langle|\psi_6|\rangle \approx 0.69$ irrespective of the exponent of the underlying repulsive power-law potential used in the simulations. Larger values correspond to hexatic or solid phases (respectively their onsets), while smaller values are characteristic for liquid phases. For details, we refer the reader to Supporting Information.

Figure 1b shows $\langle|\psi_6|\rangle$ of the skyrmion lattice at fixed out-of-plane field and sample temperature as a function of time after the initial lattice nucleation. As visible, the angular ordering as well as translational ordering as quantified by the pair correlation function (Figure 1c) is not constant instantly after switching off the magnetic in-plane field: A local liquid-like structure emerges and becomes more pronounced as relaxation proceeds. Note that it is not possible to distinguish the 1D $g(r)$ of the hexatic phase from that of a dense liquid as pointed out above. Immediately after switching off this field, the skyrmions are nucleated on a timescale that is below the time resolution of the measurement setup (ms). This is then followed by a stabilization phase in the range of seconds to tens of seconds. The stabilization time frame is influenced by the energy landscape of the multilayer material and the diffusion parameter of the skyrmions to form an ordered structure that we term here in line with literature a skyrmion lattice. While the initial ordering occurs rather quickly in all cases, $\langle|\psi_6|\rangle$ is still increasing slightly over the course of our measurement (60 s) consistent with the expected prolonged equilibration times associated with the emergence of hexagonal order. We refer to the last 30s of the $\langle|\psi_6|\rangle(t)$ as the "semi-steady" state, which is a sufficiently long period to robustly measure quantifiers. The initial 4 s after switching off the in-plane field where the highest slope of $\langle|\psi_6|\rangle(t)$ is found and where the nucleated skyrmions form a lattice is referred to as the "nucleation" period. The "relaxation" period covers the remaining part of the time evolution. These criteria were chosen by comparing the obtained videos at every temperature and out-of-plane field combination for a comparable evaluation of the skyrmion lattice.

While as shown in Figure 1b, at 338 K the system orders with $\langle|\psi_6|\rangle > 0.69$ (indicating possibly a hexatic phase, see further below for a detailed discussion), at 330 K $\langle|\psi_6|\rangle$ only goes up to the value of 0.55, consistent with the formation of a more disordered dense liquid phase. Likewise, the pair correlation function also changes in the course of equilibration (Figure 1c). Fluctuations are related to the thermally activated movement of the skyrmions that occurs in the lattice. We observe that skyrmions repel each other and we do not see any significant skyrmion-skyrmion annihilation thus boding well to study the phase transitions. Having established the time evolution of $\langle|\psi_6|\rangle$, we now systematically study the dependence of the semi-steady state lattice properties on the external parameters, temperature and magnetic field to explore the tunability. The average $\langle|\psi_6^t|\rangle$ is obtained from all frames after 30 s of equilibration and shown in **Figure 2**. With reducing temperature, the range of out-of-plane field where skyrmions can be stabilized becomes narrower and a monotonic trend of higher hexagonal order with higher temperature is observed. The highest temperature achievable was limited by the measurement temperature control as well as the spatial resolution since the skyrmion diameter depends on temperature. At too low out-of-plane fields, after in-plane field sweeps, not only skyrmions are stabilized but also elongated chiral domains are present. These effectively distort the lattice and hinder its higher ordering so

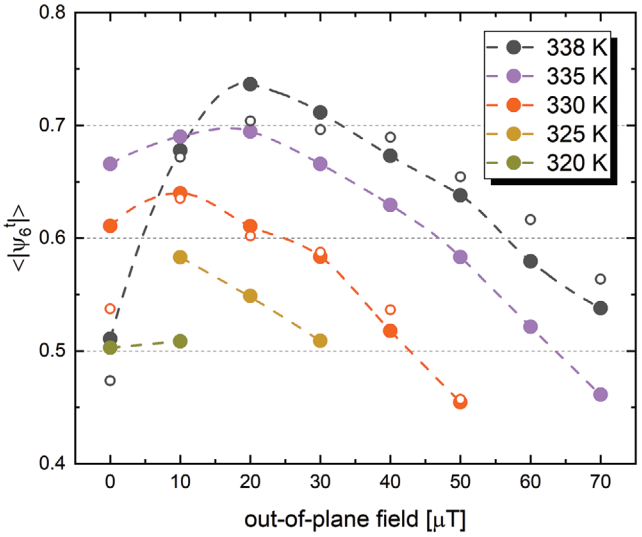

Figure 2. Time averaged $\langle|\psi_6^t|\rangle$ for different out-of-plane fields in the temperature range 325–338 K. The field and temperature ranges are limited by the stability of a pure skyrmion lattice as well as the minimum size of skyrmions that can be detected. The highest ordering achieved is at 338 K with 20 μT. $\langle|\psi_6^t|\rangle$ was calculated from the skyrmion position in the sample in the semi-steady state part of the skyrmion lattice formation (after 30 s since the skyrmion nucleation). Empty circles are simulation results corresponding to $T = 338$ K and $T = 330$ K and were determined after 10^6 simulation time steps. Dashed lines serve as guidelines between points only.

that we have focused on parameter combinations where we have only skyrmions. A decreasing tendency of angular order is found at increased out-of-plane field values for every studied temperature. This can result from higher skyrmion-skyrmion distances, where the thermal movement of the magnetic textures is more pronounced and thus hinders the ordering of the lattice. A maximum value of $\langle|\psi_6^t|\rangle$ of around 0.73 is obtained at the highest investigated temperature and 20 μT out-of-plane field when also the highest observable skyrmion density is reached.

As the onset of the hexatic (or even solid) phase is directly visible in the spatially resolved map of the local orientational order parameter, we study this at the maximum value of $\langle|\psi_6^t|\rangle$ (338 K, 20 μT): **Figure 3**a shows the hexatic skyrmion domains with coincident orientation of ψ_6 as measured by the angle θ (Euler angle of the complex number ψ_6 divided by 6 as explained in Section 4). The average domain size is of the order of 50 μm, corresponding to roughly 100 skyrmions. In particular we see a homogenous distribution of $|\psi_6|$ in Figure 3c.

For comparison, we also show the corresponding liquid phase results for $T = 330$ K and B = 40 μT in Figure 3b,d). Note that skyrmions are much larger under these conditions and domains of similar orientation are of the order of 10 particles or less. In this liquid phase, there is no homogeneous distribution of $|\psi_6|$ as shown by the irregular colors in Figure 3d. To understand our results and draw robust conclusions about the phases and the 2D nature of the studied system, we support the experimental results with numerical simulations using a model of soft particles which interact with each other via a repulsive power-law potential r^{-n}. This choice is purely empirical but allows us to describe the strong short range repulsive interaction studied previously.[26] At the same time, the chosen potential benefits from the availability of exact phase diagrams for a wide range of n.[18] For $n \geq 6$ (which includes the hard disk scenario) the transition from the liquid to the hexatic phase was shown to be of first order followed by a continuous transition to

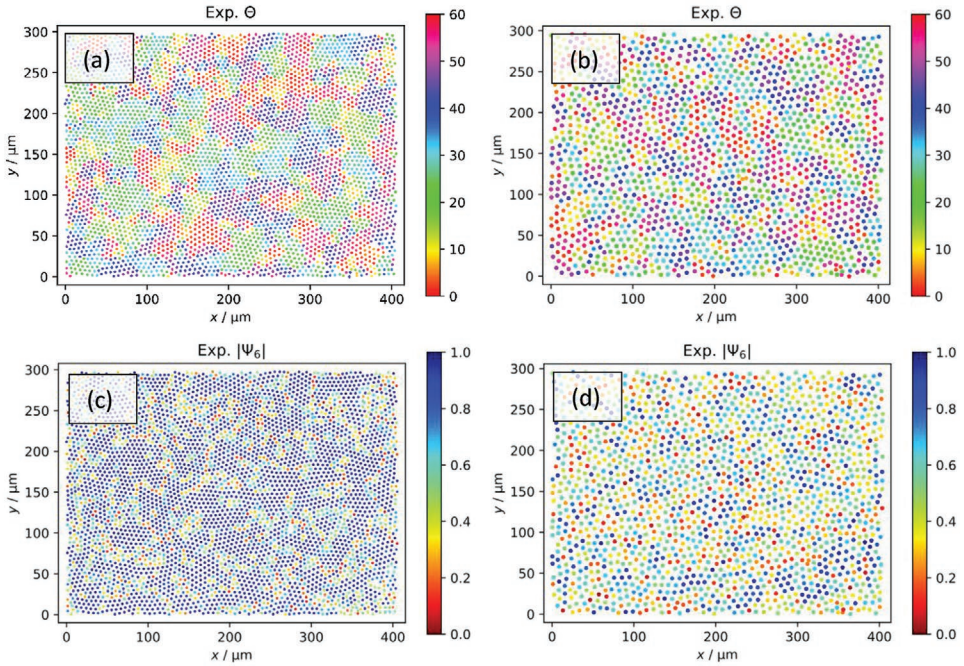

Figure 3. Spatial distribution of the local orientational order parameter ψ_6 of individual skyrmions. (a) and (c) were evaluated at 338 K and an out-of-plane field value of 20 μT. This represents the state with the highest value of $\langle|\psi_6^t|\rangle$ in Figure 2. (a) visualizes the orientation of ψ_6, that is, the orientation angle θ, while (c) visualizes the absolute value of ψ_6. (b) and (d) are corresponding figures for 330 K and 40 μT.

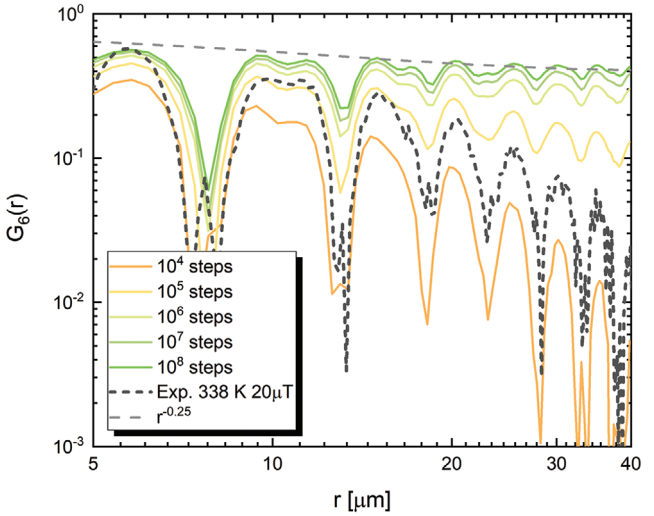

Figure 4. Decay of the spatial correlation function G_6 for the experimental system (338 K, 20 μT, averaged over frames 300–960) and matching simulations after different runtimes (single snapshot of a quadratic simulation box containing 40 000 particles).

the solid phase.[18] For smaller values of n, the transition from the liquid to the hexatic phase becomes continuous and of the Kosterlitz-Thouless–Halperin–Nelson–Young (KTHNY) type.[27]

In the following, we want to ascertain to which extent skyrmion lattices can be used as generic model systems to explore the phase behavior of 2D systems akin to colloids.[21–23] At the same time, we want to gauge if a coarse phenomenological model from statistical physics is actually able to describe the bulk macroscopic behavior of skyrmions accurately. Building upon expansive numerical work, which has determined the phase behavior of soft disks with great accuracy, Molecular Dynamics simulations of this model were performed and mapped onto our skyrmion system.[18,28–30] Parameters were adjusted to match the pair correlation function of skyrmions for a given density. Note that fixing n (to, e.g., 6 to represent interactions between dipoles) will generally lead to a worse agreement with the experimental $g(r)$. For a detailed discussion of the mapping procedure, see Section 4 and Supporting Information.

Using this ansatz, we have reproduced the experimentally observed behavior of $\langle|\psi_6^t|\rangle$ for $T = 338$ K and $T = 330$ K (Figure 2). Qualitative agreement between simulations and experiments is found. However, one should note that $\langle|\psi_6|\rangle$ is very sensitive to the details of the mapping (e.g., if all details or only parts of $g(r)$ are used). Another caveat for both simulations and experiments at $T = 338$ K is the time after which $\langle|\psi_6|\rangle$ is measured as it increases during the course of equilibration. Nevertheless, considering that our mapping is purely based on basic structural information (namely density and the 1D $g(r)$), the qualitative agreement shows that static properties of skyrmion interactions can indeed be captured by a coarse-grained phenomenological model.

A more quantitative approach relies on the decay of the spatial correlation function G_6 which can also be used to distinguish phases in 2D systems:[21,22]

$$G_6(r) = \frac{1}{n_r} \sum_{|r_k - r_l| = r} \psi_6(r_k)\psi_6^*(r_l) \tag{3}$$

Here, we sum over all n_r particle pairs whose distance is r. In **Figure 4**, we compare the decay of G_6 from experiment at $T = 338$ K and B = 20 μT and simulation. While this correlation function decays exponentially in the liquid phase, quasi-long range orientational order is expected to emerge in the hexatic phase.[27] Depending on the equilibration time after which the correlation function is measured in the simulation, the envelope of G_6 increases toward an algebraic decay. We also observe that the experimental data (black dashed curve) is still decaying exponentially and is likely not fully equilibrated, yet, in line with our observations in Figure 3a.

The effect of equilibration can also be seen in simulation snapshots. While after 10^4 equilibration steps the distribution of θ in **Figure 5**a (as well as the decay of G_6) is similar to the corresponding experimental plot (Figure 3a), the domains of similar orientation continue to grow as indicated by a snapshot taken after 10^8 equilibration steps (Figure 5b).

3. Conclusions

Based on our numerical simulations, we conclude that the observation of multiple domains in the experiment (Figure 3) is likely the result of an incomplete equilibration process as equilibration times are notoriously large in an emergent hexatic (or solid) phase. This is corroborated by the observation that

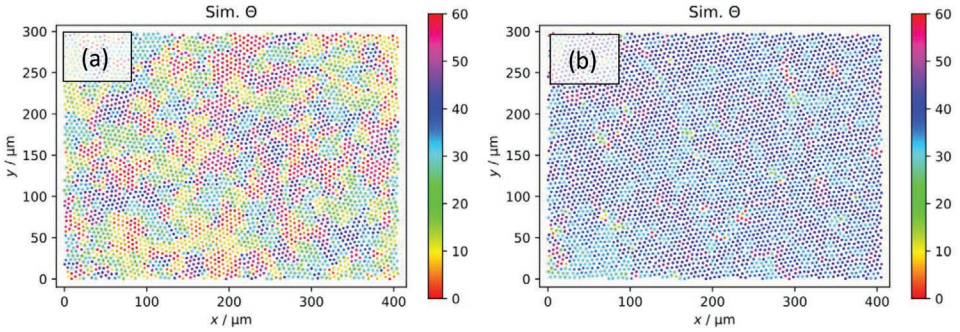

Figure 5. Spatial distribution of θ in a simulation corresponding to a sample temperature of 338 K and an out-of-plane field of 20 μT after a) 10^4 and b) 10^8 equilibration steps. Only a small part of the simulation box is shown to make plots comparable to Figure 3a.

the sizes of the experimental domains continue to grow up to the maximum time which can be measured (that is limited by the setup stability). Additionally, we occasionally see structural defects that pin certain skyrmions that are thus not ordered locally and remain unordered potentially leading to artificial domain wall pinning.

In conclusion, we have analyzed the phases of skyrmion lattices to identify the reduced dimensionality of this µm sized but sub-nm thick system. We have shown that by using the pair correlation function and local orientational order parameter we can characterize the skyrmion lattice system, which allows us to investigate 2D phase transitions. Temperature and out-of-plane field impact density and mean skyrmion-skyrmion distance and translate to different nucleation dynamics and hexagonal ordering of the observed lattice. We find that the hexagonal order increases with higher temperature and field values in the range of 10–30 µT. Above 338 K, the skyrmion lattice cannot be resolved with the optical microscope setup. For the majority of the selected parameters, we observe behavior consistent with a 2D, dense liquid. However, we also find that for selected conditions, our system is in an emergent hexatic (or even solid) phase showing its 2D nature. As expected for the hexatic phase, we find that the equilibration in this phase is very slow. By comparison with theory, we were able to reproduce qualitatively the experimentally observed phase behavior using computer simulations with a simple phenomenological model based on soft disks by matching density and the 1D pair correlation function. We thus demonstrate that static behavior of skyrmion ensembles may be described by a simple 2D model system highlighting that our skyrmion lattices can indeed be used as 2D model systems with major advantages in terms of tunability and speed compared to conventionally used 2D model systems such as colloids.

4. Experimental Section

Sample Parameters: The sample was prepared using magnetron sputtering in a Singulus Rotaris sputtering tool. The base pressure during the growth process was less than 3×10^{-8} mbar. The composition of the single stack was $Ta(5)/Co_{20}Fe_{60}B_{20}(0.9)/Ta(0.08)/MgO(2)/Ta(5)$, with the thickness of individual layers given in nanometers in parentheses. With the used deposition system, the thickness of the individual layers can be tuned in the stack in a controlled manner with high accuracy. The stack is similar to the one reported on previously where it was found that the very thin Ta layer on top of the CoFeB plays a key role in setting the effective anisotropy.[11] The sample was characterized using the magneto-optical Kerr effect (MOKE) measurement. Single skyrmions can be stabilized in the ferromagnetic layer using out-of-plane field sweeping, meaning applying an oscillating out-of-plane field over several oscillation periods. This procedure moves the domains and eventually they break into smaller domains and in this case can form skyrmions. Elongated domains and skyrmions exhibit thermally activated diffusion. The hysteresis loop in applied out-of-plane field shows an hour-glass shape, typical for material with the presence of skyrmions (see Supporting Information). With higher temperature, the hysteresis loop is tilted toward larger applied fields. This indicates a change of the anisotropy of the material with temperature. The lowest investigated temperature is determined by the ability to stabilize the skyrmion lattice. Below 325 K, only stripe domains were nucleated by the saturation of the sample with an in-plane field. The highest achievable temperature for the lattice investigation was determined by the resolution of the microscope and the thermally activated motion of skyrmions. Above 338 K, the size of the skyrmions was comparable to the resolution of the Kerr microscope. The skyrmions movement was also more rapid. Above this temperature, no reliable skyrmion tracking in this material system could be performed.

The DMI was measured by investigating the domain periodicity at zero magnetic field and by comparison with micromagnetic simulations. Using the measured parameters of magnetic anisotropy and saturation magnetization and an exchange parameter of $A = 10$ pJ m^{-1}, it was found that DMI is needed to stabilize skyrmion structures. The obtained DMI from comparing the measurement with the simulations is comparable to the value published previously for a similar stack ($D_I = 0.3 \pm 0.1$ mJ m^{-2}).[11] The DMI in the material is sufficiently strong so that only topologically non-trivial skyrmion spin structures are stable. The effect of the topology on the skyrmion lattice phases and phase transitions could be studied in a material where both topologically trivial bubbles and non-trivial skyrmions are stable, which however goes beyond the scope of the current work.

Measurement Setup: A commercial Evico GmbH MOKE microscope was used. The optical spatial resolution is approximately 400 nm. The temporal resolution remains the same at any temperature and magnetic field and is 62.5 ms. At higher temperatures, the skyrmions become much smaller and their diffusion is enhanced and thus faster. This hinders the reliable tracking to identify the position given the time resolution. Therefore, the threshold where skyrmions can be tracked is determined by both the temporal and spatial resolution of the microscope setup. The in-plane field coil was supplied from the microscope manufacturer. The highest achievable in-plane field was 300 mT. The coil for the out-of-plane field application was custom built at the University of Mainz. The coil was designed to have negligible coercivity and to be able to supply the sample with very small controlled fields in orders of µT. A current versus magnetic field calibration was performed using a Gaussmeter in the position of the sample and used during the measurement along different directions. The calibration for the Earth magnetic field was done using the hysteresis loop of the material. The residual Earth field caused an offset in the *x*-axis of the *M-H* loop. The authors compensated for this offset in the coil calibration. The calibration of all stray-fields and resulting offsets in the field values was performed before every measurement and no changes were observed during the timescale of the measurement. Adjustment of the in-plane field coil was done the same way. When the coil was tilted or set in a way that a cross field between the out-of-plane and in-plane field was present, the *M-H* loop of the material was shifted. The in-plane field coil was adjusted so that the hysteresis loop is the same as without the coil, only with out-of-plane field. A stage with two HighTech QuickCool QC-32-0.6.1.2 Peltier elements was used for the temperature change of the sample in the range of 280–350 K. The temperature was externally controlled by measurement of resistivity of a Pt100 resistor, which was placed next to the multilayer sample. The stability of the set temperature was measured to be within 0.3 K. The frame rate of the microscope camera was 16 frames s^{-1}; therefore, the time resolution of the microscope measurement was 62.5 ms.

Skyrmion Tracking: Skyrmion lattices are visualized using a Magneto-Optical Kerr-Microscope. In the pictures the out-of-plane magnetization is represented by a grey scale, so that the skyrmions appear as light blobs on a dark(er) background. Videos recorded that way were consecutively analyzed using the Trackpy[31] package. In a first stage, it locates the skyrmions by detecting Gaussian-like blobs in the grey scale movies. It was ensured that the software finds all skyrmions in the individual video frames. Several parameters are set to optimize the recognition for reliable results. Most importantly, the mask-parameter sets a rough estimate for the pixel-diameter of the features to be found. During the evaluation, it is set slightly above the average skyrmion diameter determined by simple binarization of the frame. The separation-parameter enforces a minimum separation between the recognized features, this way over-recognition in defective areas is prevented. A safe value for the recognition is several pixels lower than the average skyrmion distance. The percentile-parameter depends on the contrast of the video and indicates to which extend the features are expected to be brighter than the surrounding area. The noise-parameter is a measure for the "sharpness" of the features to be detected and can vary between

measurement videos with different external parameters. Most of the skyrmion diameters are in a range from 7 to 13 pixels, corresponding to 4.5–8.5 μm. For example, at the temperature of 338 K and the out-of-plane field of 20 μT, we set the mask to 9, the separation to 4, and the noise to 0.15.

Quantifiers for Phase Transitions in 2D Systems: The pair correlation function (PCF) (Equation (2)) determines the probability of finding two skyrmions at a distance **r** from each other. The position of the first peak assesses the mean nearest neighbor distance and deep in the solid phase characteristic sharp peaks resulting from the underlying lattice appear. It is, however, impossible to distinguish $g(r)$ of liquid, hexatic and solid phases close to the phase transition and other identifiers need to be considered. Since the disk-shaped skyrmions develop hexagonal order as the bulk density increases, one can resort to the local orientational order parameter ψ_6 (Equation (1)).[27] This complex parameter measures deviations from hexagonal order. The absolute value $|\psi_6| = 1$ for a perfect triangular lattice and decreases to 0 with increasing disorder. In addition to the absolute value of ψ_6 one can also extract the local orientation angle of neighboring skyrmions, that is, the Euler angle of ψ_6 divided by 6. Note that the orientation of a hexagonally ordered cluster consisting of the central particle and its six neighbors is essentially determined by the angle between the *x*-axis and the vector of the central particle and its neighbor in the range of 0–60°. The factor of six in the definition of ψ_6 projects all vectors between the central particle and its neighbors on top of each other and ψ_6 averages over these projections. The orientation angle (ranging from 0° to 60°) is therefore a gauge for the local orientation of the cluster with respect to the *x*-axis. This parameter is well-suited to visualize clusters of equal orientation. In simulations of soft disks, it was also noticed empirically that the mean $|\psi_6|$ is roughly $\langle|\psi_6|\rangle \approx 0.69$ at the liquid branch of the liquid to hexatic phase transition (see Supporting Information), and this parameter was used as an additional indicator for the transition. For computing $g(r)$ and ψ_6, the MD analysis program FREUD was employed.[17]

Molecular Dynamics Simulations of Soft Disks: Molecular Dynamics simulations of soft disks were performed using the model of Kapfer and Krauth with the HOOMD Molecular Dynamics package and a Langevin integrator:[18,32]

$$V(r) = \left(\frac{\sigma}{r}\right)^n \tag{4}$$

In this coarse, phenomenological model for the bulk behavior of skyrmions, σ roughly corresponds to the mean skyrmion distance, and n denotes the steepness of the potential. By running MD simulations at the experimentally determined skyrmion density, the authors were able to adjust the simulation potential so that the pair correlation for the simulated soft disks matches the pair correlation of the skyrmions. In order not to overparameterize the mapping to the experimentally measured PCFs, the authors only adjusted n and set σ constant. Even though the position of the first peak of the PCFs is not necessarily identical with the σ of the simulation potential, this approximation turns out to be sufficiently accurate for the examined densities. Therefore, σ was set in the simulations to be the position of the first peak of the experimentally determined PCFs. Simulations were then run for varying n in the range between 6 and 12 with 0.1 resolution. The matching of the simulated and experimental PCFs is determined as mean squared deviation measured up to the fourth maximum. This deviation shows a smooth dependence of n and a clear minimum which were taken as best match to the experiment. The optimal n is typically around 10 (for $T = 338$ K) and somewhat lower for lower temperatures. The determined density, σ and n allow running simulations mapped closely to the experiment and the estimated underlying experimental potential. For these mapped simulations, the mean absolute value $\langle|\psi_6|\rangle$ were determined, which is to some extent, dependent on the equilibration time of the simulations. If not mentioned otherwise, the system was equilibrated for 10^6 time steps before measurements were taken. It should also be noted that the simulations employ a Langevin dynamics thermostat with a time step of 10^{-3} and could be further improved by including additional specific terms to account for gyrotropic dynamics.[33–35] It is not expected that the current static equilibrium results are affected because such terms do not contribute to the energy of the system and thus do not break detailed balance.[35] However, to analyze the dynamics of the system evolution in the future, such terms need to be considered.

Data Availability

The data that support the plots within this paper and other findings of this study are available from the corresponding author upon reasonable request.

Supporting Information

Supporting Information is available from the Wiley Online Library or from the author.

Acknowledgements

The authors would like to thank Kurt Binder for insightful discussions and acknowledge funding from TopDyn, SFB TRR 146, SPP 1726, and SFB TRR 173 Spin+X (project A01). The experimental part of the project was additionally funded by the Deutsche Forschungsgemeinschaft (DFG, German Research Foundation) project No. 403502522 (SPP 2137 Skyrmionics) and the EU (3D MAGIC ERC-2019-SyG 856538, s-NEBULA H2020-FETOPEN-2018-2020 863155).

Open access funding enabled and organized by Projekt DEAL.

Conflict of Interest

The authors declare no conflict of interest.

Author Contributions

J.Z. and F.D. contributed equally to this work. M.K., P.V., and J.Z. proposed and supervised the study. J.Z. and N.K. fabricated and characterized the multilayer samples. J.Z., N.K., and K.R. prepared the measurement setup and conducted the experiments using the Kerr microscope. F.D., J.Z., Y.G., T.W., and N.K. evaluated the experimental data with the help of K.R., P.V., M.V., and K.L. F.D. and P.V. conducted theoretical simulations and comparison with the experimental results. J.Z. and F.D. prepared the manuscript with the help of M.V., P.V., and M.K. All authors commented on the manuscript.

Keywords

2D phase transitions, hexatic phase, skyrmion lattice, skyrmion-skyrmion interactions

Received: May 9, 2020
Revised: July 17, 2020
Published online: September 3, 2020

[1] A. Fert, N. Reyren, V. Cros, *Nat. Rev. Mater.* **2017**, *2*, 17031.
[2] G. Finocchio, F. Büttner, R. Tomasello, M. Carpentieri, M. Kläui, *J. Phys. D. Appl. Phys.* **2016**, *49*, 423001.
[3] X. Zhang, M. Ezawa, Y. Zhou, *Sci. Rep.* **2015**, *5*, 9400.

[4] F. Jonietz, S. Mühlbauer, C. Pfleiderer, A. Neubauer, W. Münzer, A. Bauer, T. Adams, R. Georgii, P. Böni, R. A. Duine, K. Everschor, M. Garst, A. Rosch, *Science* **2010**, *330*, 1648.
[5] X. Z. Yu, N. Kanazawa, W. Z. Zhang, T. Nagai, T. Hara, K. Kimoto, Y. Matsui, Y. Onose, Y. Tokura, *Nat. Commun.* **2012**, *3*, 988.
[6] W. Jiang, P. Upadhyaya, W. Zhang, G. Yu, M. B. Jungfleisch, F. Y. Fradin, J. E. Pearson, Y. Tserkovnyak, K. L. Wang, O. Heinonen, S. G. E. E. te Velthuis, A. Hoffmann, *Science* **2015**, *349*, 283.
[7] S. Woo, K. Litzius, B. Krüger, M.-Y. Im, L. Caretta, K. Richter, M. Mann, A. Krone, R. M. Reeve, M. Weigand, P. Agrawal, I. Lemesh, M.-A. Mawass, P. Fischer, M. Kläui, G. S. D. D. Beach, *Nat. Mater.* **2016**, *15*, 501.
[8] I. Lemesh, K. Litzius, M. Böttcher, P. Bassirian, N. Kerber, D. Heinze, J. Zázvorka, F. Büttner, L. Caretta, M. Mann, M. Weigand, S. Finizio, J. Raabe, M. Im, H. Stoll, G. Schütz, B. Dupé, M. Kläui, G. S. D. Beach, *Adv. Mater.* **2018**, *30*, 1805461.
[9] F. Zheng, H. Li, S. Wang, D. Song, C. Jin, W. Wei, A. Kovács, J. Zang, M. Tian, Y. Zhang, H. Du, R. E. Dunin-Borkowski, *Phys. Rev. Lett.* **2017**, *119*, 197205.
[10] K. Everschor-Sitte, J. Masell, R. M. Reeve, M. Kläui, *J. Appl. Phys.* **2018**, *124*, 240901.
[11] J. Zázvorka, F. Jakobs, D. Heinze, N. Keil, S. Kromin, S. Jaiswal, K. Litzius, G. Jakob, P. Virnau, D. Pinna, K. Everschor-Sitte, L. Rózsa, A. Donges, U. Nowak, M. Kläui, *Nat. Nanotechnol.* **2019**, *14*, 658.
[12] D. Prychynenko, M. Sitte, K. Litzius, B. Krüger, G. Bourianoff, M. Kläui, J. Sinova, K. Everschor-Sitte, *Phys. Rev. Appl.* **2018**, *9*, 014034.
[13] T. Nakajima, H. Oike, A. Kikkawa, E. P. Gilbert, N. Booth, K. Kakurai, Y. Taguchi, Y. Tokura, F. Kagawa, T. Arima, *Sci. Adv.* **2017**, *3*, e1602562.
[14] S. Mühlbauer, B. Binz, F. Jonietz, C. Pfleiderer, A. Rosch, A. Neubauer, R. Georgii, P. Böni, *Science* **2009**, *323*, 915.
[15] P. Huang, T. Schönenberger, M. Cantoni, L. Heinen, A. Magrez, A. Rosch, F. Carbone, H. M. Rønnow, *Nat. Nanotechnol.* **2020**, 1, https://doi.org/10.1038/s41565-020-0716-3.
[16] S. A. Díaz, C. J. O. Reichhardt, D. P. Arovas, A. Saxena, C. Reichhardt, *Phys. Rev. B* **2017**, *96*, 085106.
[17] V. Ramasubramani, B. D. Dice, E. S. Harper, M. P. Spellings, J. A. Anderson, S. C. Glotzer, *Comput. Phys. Commun.* **2020**, *254*, 107275.
[18] S. C. Kapfer, W. Krauth, *Phys. Rev. Lett.* **2015**, *114*, 035702.
[19] M. Engel, J. A. Anderson, S. C. Glotzer, M. Isobe, E. P. Bernard, W. Krauth, *Phys. Rev. E* **2013**, *87*, 042134.
[20] E. P. Bernard, W. Krauth, *Phys. Rev. Lett.* **2011**, *107*, 155704.
[21] K. Zahn, R. Lenke, G. Maret, *Phys. Rev. Lett.* **1999**, *82*, 2721.
[22] K. Zahn, G. Maret, *Phys. Rev. Lett.* **2000**, *85*, 3656.
[23] P. Keim, G. Maret, H. H. Von Grünberg, *Phys. Rev. E* **2007**, *75*, 031402.
[24] Y. Nishikawa, K. Hukushima, W. Krauth, *Phys. Rev. B* **2019**, *99*, 064435.
[25] P. Dillmann, G. Maret, P. Keim, *J. Phys. Condens. Matter* **2012**, *24*, 464118.
[26] U. K. Rößler, A. A. Leonov, A. N. Bogdanov, *J. Phys. Conf. Ser.* **2011**, *303*, 012105.
[27] D. R. Nelson, B. I. Halperin, *Phys. Rev. B* **1979**, *19*, 2457.
[28] J. Zausch, P. Virnau, K. Binder, J. Horbach, R. L. Vink, *J. Chem. Phys.* **2009**, *130*, 064906.
[29] D. Winter, J. Horbach, P. Virnau, K. Binder, *Phys. Rev. Lett.* **2012**, *108*, 028303.
[30] S. K. Das, S. A. Egorov, B. Trefz, P. Virnau, K. Binder, *Phys. Rev. Lett.* **2014**, *112*, 198301.
[31] Trackpy, https://github.com/soft-matter/trackpy (accessed: July 2019).
[32] J. A. Anderson, C. D. Lorenz, A. Travesset, *J. Comput. Phys.* **2008**, *227*, 5342.
[33] A. A. Thiele, *Phys. Rev. Lett.* **1973**, *30*, 230.
[34] B. L. Brown, U. C. Täuber, M. Pleimling, *Phys. Rev. B* **2018**, *97*, 020405.
[35] B. L. Brown, U. C. Täuber, M. Pleimling, *Phys. Rev. B* **2019**, *100*, 024410.